Publications of the Astronomical Society of Australia (2021), 1–4
doi:10.1017/pasa.xxxx.xx

CAMBRIDGE
UNIVERSITY PRESS

Research Paper

Discovery of an Extremely Metal-Poor Galaxy at $z = 3.654$ using JWST infrared spectroscopy

Zijian Yu[1] and Sijia Cai[2]

[1]Blair Academy, 2 Park St, Blairstown, New Jersey 07825 [2]Department of Astronomy, Tsinghua University, Beijing 100084, China

Abstract

We report the discovery of an extremely metal-poor galaxy at a redshift of $z = 3.654$, identified through infrared spectroscopy using the James Webb Space Telescope (JWST). This galaxy, CAPERS-39810, exhibits a metallicity of $12 + \log(\mathrm{O/H}) = 6.79^{+0.17}_{-0.23}$, indicative of its primitive chemical composition, resembling the early stages of galaxy formation in the Universe. We utilized JWST's NIRSpec/MSA for spectroscopic analysis, complemented by photometric data from the COSMOS2025 catalog. Our analysis employs the R3 strong-line diagnostic method to estimate metallicity, due to the lack of auroral lines in the spectrum. The galaxy's emission lines, including Hβ, [OIII], and HeI, are clearly detected, with the rest-frame equivalent width of 195 ± 63, 354 ± 95, and 130 ± 52 Å, respectively. Furthermore, we perform detailed SED modeling to derive a galaxy logarithmic stellar mass of $8.10^{+0.22}_{-0.30}\ M_{\odot}$. This discovery adds to the growing body of evidence for the existence of very low-metallicity galaxies existed at cosmic noon of $z \approx 3$, which are crucial for understanding the processes of chemical enrichment and star formation in young galaxies at the cosmic noon.

Keywords: Key1, Key2, Key3, Key4

(Received xx xx xxxx; revised xx xx xxxx; accepted xx xx xxxx)

1. Introduction

At the beginning, the universe contained almost no metals at all—only hydrogen, helium, and tiny traces of lithium left over from Big Bang nucleosynthesis. The first stars — population III (Pop-III) stars — were born from this pristine gas. Because no metals existed to efficiently cool the gas, theory predicts these stars to have grown extraordinarily massive. Due to their immense masses, their fuel depleted rapidly and their lives ended violently, either as pair-instability supernovae or core-collapse supernovae. These explosions forged and expelled the very first metals into the surrounding medium, kicking off the chemical enrichment of the universe (e.g., Bromm & Larson 2004; Bromm & Yoshida 2011). Because these primordial stars can no longer be directly observed, the closest we can get to studying them is by searching for and analyzing extreme metal-poor galaxies (EMPGs), which serve as crucial laboratories to study physical conditions and processes similar to those of the primordial universe, helping us uncover the earliest chapters of cosmic evolution (e.g., Izotov et al. 2018; Kojima et al. 2020; Isobe et al. 2022; Nakajima et al. 2022).

Although no direct observations of Pop-III stars have been made to date, their existence is supported by a convergence of cosmological models, indirect observations, and nucleosynthetic evidence. Many previous efforts have attempted to search for the elusive Pop-III stars through analysis of extreme metal-poor galaxies. One widely used approach is to analyze EMPGs, whose low gas phase abundances can preserve signatures of early chemical enrichment (Izotov et al., 2018; Kojima et al., 2020; Isobe et al., 2022). The metallicities in these systems are traditionally derived from rest-frame optical spectroscopy obtained from facilities such as Subaru/FOCAS and Keck/MOSFIRE. The advent of JWST NIRSpec has revolutionized this field, as it enables rest-frame optical spectroscopy of faint galaxies at high redshifts across reionization and cosmic noon (e.g., Sanders et al. 2024; Casey et al. 2023 the COSMOS-Web contexts). The most robust and accurate estimates rely on the direct "Te" method, which uses detections of faint auroral lines such as [OIII] λ4363 along with strong nebular lines such as [OIII] $\lambda\lambda$4959, 5007 to constrain electron temperature and thus ionic abundances (e.g., Sanders et al. 2020; Chakraborty et al. 2025; Scholte et al. 2025). When auroral lines are unavailable, auroral-strong line calibrations — "empirical" methods — are usually the next option. Empirically or theoretically mapping ratios of bright collisionally excited line ratios such as R23, O3N2, and N2 are mapped to metallicities anchored by direct Te measurements, thereby enabling metallicity estimations in systems where auroral lines are undetected, although they usually introduce larger systematic uncertainties–especially at lower metallicities (e.g., Nakajima et al. 2022; Sanders et al. 2024). Sometimes, recombination line (e.g., [OII] λ4650, [CII] λ4267) methods can be used, providing abundance estimates less sensitive to gas-phase electron temperatures. Despite it often being used as a "gold standard" for comparison to other metallicity calibrations, it still holds the main disadvantage that recombination lines are extremely faint and rarely detected. Finally, theoretical diagnostics derived from photoionization models (e.g., CLOUDY-based grids, Starburst99 stellar evolution models) can be employed to infer physical conditions of ionized gas through comparison of emission line fluxes. Oxygen is typically adopted as the benchmark for

Author for correspondence: A. Cambridge, Email: ACambridge@student.unimelb.edu.au

Cite this article: Author1 C and Author2 C, an open-source python tool for simulations of source recovery and completeness in galaxy surveys. *Publications of the Astronomical Society of Australia* **00**, 1–12. https://doi.org/10.1017/pasa.xxxx.xx

metallicity given its nucleosynthetic origins and the accessibility of strong [OIII] and [OII] transitions, while complimentary ratios such as C/O, N/O, and Fe/O are also examined to trace enrichment pathways, a characteristic of Population III.

Beyond nebular oxygen abundances, additional strategies may include exploiting ionizing radiation or rest-frame UV diagnostics. One of the most direct probes is the Lyman continuum (LyC) leakage, indirectly traced via Lyα and related diagnostics, provides constraints on whether low-Z galaxies could supply the ionizing photons required for reionization (e.g., Stark 2016). However, direct LyC detections are severely limited at higher redshifts as they are strongly attenuated by the intergalactic medium (IGM), so indirect tracers are often employed. The Lyman-α (Lyα) emission line serves as one such method: as its strength and profile heavily depend on metallicity, dust, and geometry of neutral hydrogen, as strong Lyα emitters are often found among EMPGs.

Another strategy focuses on the detection of HeII λ1640, a recombination line expected to be produced by hard ionizing spectra from very massive, extremely metal-poor stellar populations. While detections of nebular HeII have been reported in both local and high-redshift EMPGs, unambiguous attribution to Pop-III stars still remain elusive, as many alternative ionization sources, such as X-ray binaries, fast radiative shocks, or AGN activity, may also produce He II (Schaerer 2003; Senchyna et al. 2017; Nanayakkara et al. 2019). The HeII λ1640 discussion is a necessary yet insufficient Pop-III indicator alone. Nevertheless, the combination of low metallicity, strong Lyα, high ionization lines, and HeII emission have increasingly started to become useful diagnostics in the search for the first stars.

In this work, we report the discovery of a candidate extreme metal-poor galaxy at z=3.654 with 12+log(O/H) = 6.77$\sim$7.15 and analyze its spectroscopy and SED to assess metallicity and physical conditions, placing it among the growing population of chemically primitive systems that JWST has so far uncovered (e.g., Willott et al. 2025; Cullen et al. 2025; Hsiao et al. 2025; Vanzella et al. 2025; Morishita et al. 2025; Mondal et al. 2025; Sanders et al. 2024). This paper is organized as follows: In Section 2, we describe our observations, including data selection and processing. In Section 3, we present our procedures for emission line flux measurements, SED fitting, and metallicity calibrations based on strong-line diagnostics. Discussion and a summary of our major conclusions are detailed in Section 4.

2. Observations and Data Processing

CAPERS-39810 is located in the well-known Cosmic Evolution Survey (COSMOS; Scoville *et al.* 2007) field at RA = 150.1335857 and Dec = 2.271014. In this work, we primarily use imaging and spectroscopic data obtained with the JWST.

2.1. Spectroscopy

The NIRSpec/MSA spectrum of CAPERS-39810 was acquired under the JWST Cycle 3 program CANDELS-Area Prism Epoch of Reionization Survey (CAPERS; GO#6368; PI: M. Dickinson). The main goal of CAPERS is to identify up to 10,000 spectroscopically confirmed galaxies at z $>$ 10 using the NIRSpec Prism. CAPERS-39810 was observed on 19 May 2025 with a total effective exposure time of 4.74 hours. The raw data are retrieved from the Mikulski Archive for Space Telescopes (MAST) at the Space Telescope Science Institute and processed using the official JWST pipeline[a] (software version 1.17.1; CRDS context `jwst_1322.pmap`; Bushouse *et al.* 2025). The standard Level 1 and Level 2 processing steps, including the 1/f noise correction, are applied. We perform background subtraction using the standard three-shutter nodding strategy to obtain 2D spectra. Finally, 1D spectra are extracted using a 6-pixel-wide box.

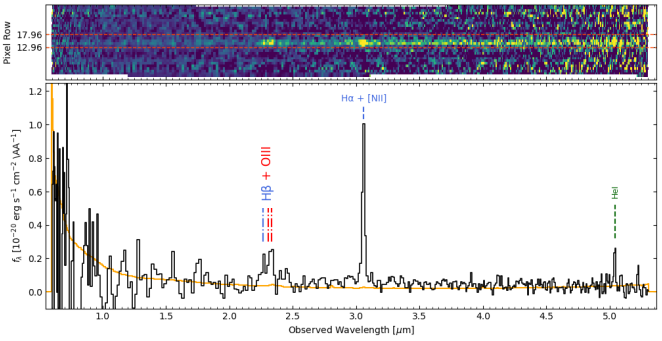

Figure 1: Spectra

2.2. Photometry

We use publicly available photometric data from the COSMOS2025 catalog (Shuntov *et al.* 2025). This includes HST/ACS F814W from the COSMOS HST ACS F814W dataset (Koekemoer *et al.* 2007), JWST/NIRCam F115W, F150W, F277W, and F444W, and JWST/MIRI F770W from the 255-hour JWST Cycle 1 Treasury Program COSMOS-Web (GO#1727; PIs: J. Kartaltepe and C. Casey; Casey *et al.* 2023). The photometry is measured in small elliptical apertures that have been corrected for Kron aperture losses and for point-spread function (PSF) effects.

3. Methods and Analysis

3.1. Emission lines

As seen in the spectrum (Figure 1), the emission lines Hα and HeI λ10830 are clearly detected. However, Hα is blended with [NII], and we therefore exclude these lines from our metallicity analysis. Due to limited spectral resolution, the two emission lines [OIII] λ4959 and [OIII] λ5007 are blended and cannot be sufficiently resolved to be distinguished as independent features. We thus model the combined [OIII] $\lambda\lambda$4959,5007 profile with a single Gaussian function. Prior to line fitting, we mask the short-wavelength region (observed wavelength $\sim$0-1.3 μm), where the noise level is high. The background continuum is modeled as a constant value, with the emission-line regions masked. Emission lines were then fitted simultaneously using a non-linear least-squares minimization routine, adopting standard Gaussian profiles to determine the line fluxes and equivalent widths (EWs).

We measure line fluxes of $f(\mathrm{H}\beta) = (4.8 \pm 1.6) \times 10^{-19}$ erg s^{-1} cm^{-2}, $f([\mathrm{OIII}]) = (8.8 \pm 2.3) \times 10^{-19}$ erg s^{-1} cm^{-2}, and $f(\mathrm{HeI}) = (3.2 \pm 1.3) \times 10^{-19}$ erg s^{-1} cm^{-2}, with a rest-frame equivalent width of $\mathrm{EW}_0(\mathrm{H}\beta) = 195 \pm 63$ Å. The measured fluxes of all detected emission lines are listed in Table 1.

[a] https://github.com/spacetelescope/jwst

3.2. Gas-phase Metallicity

The most reliable and physically motivated metallicity calibration method, the direct-T_e method, requires information on key physical conditions, such as electron temperature and electron density. However, temperature-sensitive auroral lines such as [OIII] λ4363 and OIII] λ1666 are typically faint, particularly with high-z EMPGs. As seen in our case, only the emission lines Hβ, [OIII] $\lambda\lambda$4959, 5007, and HeI λ10830 are clearly detected, with no auroral line signals. Given these limitations, we instead adopt a strong line metallicity diagnostic. Due to the low signal-to-noise ratio of the [OII] λ3727 line, other common diagnostics like $\mathrm{R23} = ([\mathrm{OII}]\lambda3727 + [\mathrm{OIII}]\lambda\lambda4959, 5007)/\mathrm{H}\beta$ do not provide meaningful constraints in this case.

We thus use the R3 extrapolation calibration defined as [OIII] λ5007/Hβ from Sanders *et al.* (2024) to determine the gas-phase metallicity. Metallicity is a function of the strong line ratio, a polynomial functional form of different orders, represented as:

$$\log(\mathrm{R3}) = 0.834 - 0.072x - 0.453x^2 \quad (1)$$

where $x = 12 + \log(\mathrm{O/H}) - 8.0$. We determine the metallicity of CAPERS-39810 to be $12 + \log(\mathrm{O/H}) = 6.79^{+0.17}_{-0.23}$.

Table 1. : **Emission Line Properties**

Parameter	Value	Unit
$f(\mathrm{H}\beta)$	$(4.8 \pm 1.6) \times 10^{-19}$	cgs [a]
$f([\mathrm{O\ III}])$	$(8.8 \pm 2.3) \times 10^{-19}$	cgs
$f([\mathrm{He\ I}])$	$(3.2 \pm 1.3) \times 10^{-19}$	cgs
R3	1.8 ± 0.8	-
$12 + \log(\mathrm{O/H})$	$6.79^{+0.17}_{-0.23}$	-
$\mathrm{EW}_0(\mathrm{H}\beta)$	195 ± 63	Å

3.3. SED modeling

We perform Spectral Energy Distribution (SED) fitting for our extreme-metal poor galaxy candidate using Bayesian Analysis of Galaxies for Physical Inference and Parameter EStimation (BAGPIPES; Carnall *et al.* 2018) to estimate its physical properties, including the approximate age and stellar mass, with the latter used to resolve the degeneracy in the strong-line metallicity calibration.

Given the very low signal-to-noise ratios (S/N) of the available spectra, we conducted the SED fitting using photometric rather than spectroscopic data. Spectroscopic fitting would not be robust for such a faint source. In our analysis, the main goal of the SED fitting is to determine whether the metallicity value inferred from strong-line calibrations corresponds to the low-mass or high-mass branch of the relation. Therefore, only approximate estimates of the stellar age and mass are required. Broad-band photometry provides sufficient constraints on these global parameters, while avoiding the additional complexity, potential systematics, and uncertainties that would arise from fitting the extremely low–S/N spectra of such a faint source.

To build the model, we adopt a Kroupa *et al.* (2002) initial mass function (IMF) and a delayed-τ star formation history (SFH):

$$\mathrm{SFR}(t) \propto t\ \exp\left(-\frac{t}{\tau}\right),$$

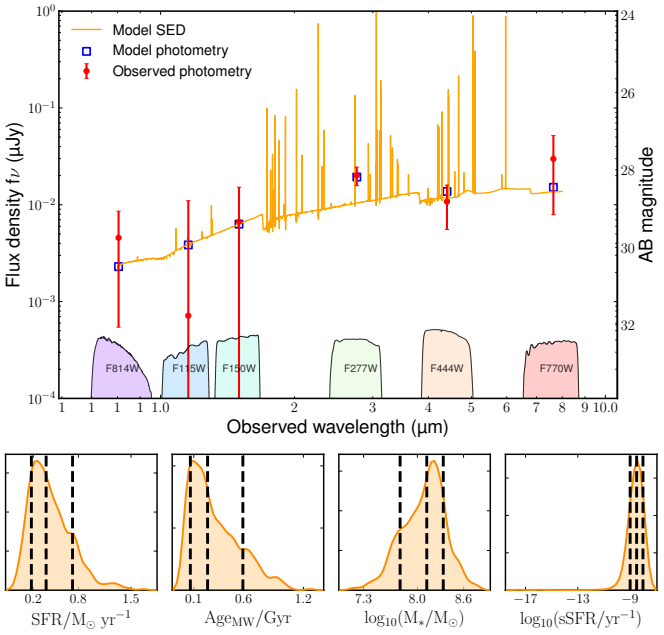

Figure 2: SED modeling of the CAPERS-39810. xxx

which describes a galaxy where star formation rate rises approximately linearly at early times ($t \ll \tau$); reaches a peak when $t \approx \tau$; and subsequently begins to decline exponentially with time, for $t \gg \tau$.

For the dust attenuation law, we adopt the flexible parametrization introduced by Salim *et al.* (2018), which extends the Calzetti *et al.* (2000) law by allowing variations in both the slope and the strength of the UV bump. We allow the attenuation curve slope, δ, to vary between –1.2 and 0.4, a range that encompasses the diversity of empirically observed attenuation curves—from steep slopes typical of starburst and low-metallicity systems ($\delta \sim -1$) to greyer attenuations seen in dusty, massive galaxies ($\delta \approx 0$–0.4). The strength of the 2175 *Å* bump, B, is allowed to vary between 0 and 2, while the total V-band attenuation, A_V, ranges from 0 to 2 mag. These wide, weakly informative priors reflect the high level of uncertainty in the observed data.

For the nebular component, we use a wide prior on the ionization parameter, $-4 < \log U < -1$, consistent with observed values in high-redshift star-forming galaxies and expected for EMPGs. The redshift is fixed to the spectroscopic value of $z = 3.654$.

The results of the SED fitting are shown in Figure 2. We report the median values of the posterior distributions along with 1σ uncertainties, corresponding to the 16th and 84th percentiles. The stellar mass is $\log_{10} M_\star/M_\odot = 8.10^{+0.22}_{-0.30}$, the age is $t_{\mathrm{age}} = 0.25^{+0.31}_{-0.18}$ Gyr, the star formation rate is $\mathrm{SFR} = 0.36^{+0.33}_{-0.17}\ M_\odot\ \mathrm{yr}^{-1}$, corresponding to a specific star formation rate of $\log_{10}(\mathrm{sSFR/yr}^{-1}) = -8.53^{+0.51}_{-0.41}$.

4. Results and Discussions

We report a dwarf galaxy, CAPERS-39810, at $z = 3.654$ in the COSMOS field, enabled by the unprecedented depth of the largest NIRSpec MSA program to date, CAPERS. This source adds a new extremely metal-poor galaxy to the intermediate-redshift sample (see Figure 3). Its NIRSpec prism spectrum shows significant detections ($\geq 3\sigma$) of Hβ, [O III] $\lambda\lambda$4959, 5007, and Hα, as well

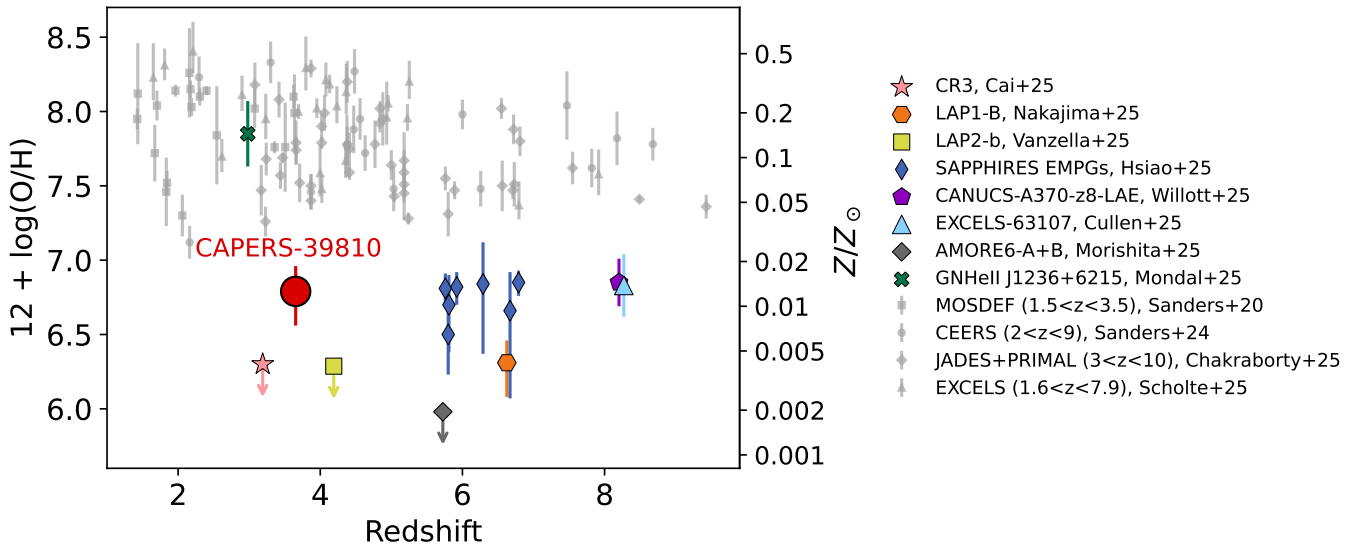

Figure 3: Gas-phase metallicity of the CAPERS-39810. For comparison, the gray markers in the figure denote the NIRSpec samples for which metallicities have been determined using the direct T_e method (Sanders *et al.* 2020; Sanders *et al.* 2024; Chakraborty *et al.* 2025; Scholte *et al.* 2025), whereas the recently reported metal-poor galaxies are highlighted with colored markers (Cai *et al.* 2025; Nakajima *et al.* 2025; Vanzella *et al.* 2025; Hsiao *et al.* 2025; Willott *et al.* 2025; Cullen *et al.* 2025; Morishita *et al.* 2025; Mondal *et al.* 2025). All upper limits in the figure are 1σ values.

as a $\sim 2.5\sigma$ detection of He I λ10830. The measured line fluxes are summarized in Table 1.

Based on the SED fitting with Bagpipes, we derive a stellar mass of $\log(M_*/M_\odot) = 8.10^{+0.22}_{-0.30}$ and a stellar population age of $0.25^{+0.31}_{-0.18}$ Myr for the target. Given its low stellar mass, we adopt the Sanders *et al.* (2024) R3 calibration and use the mass–metallicity relation to break the degeneracy between the upper and lower metallicity branches. This yields a gas-phase metallicity of $12 + \log(\mathrm{O/H}) = 6.79^{+0.17}_{-0.23}$.

Considering the known systematic uncertainties among different metallicity calibrations, it is necessary to test multiple approaches to ensure a robust metallicity estimate. Using the calibration from Nakajima *et al.* (2022), whose sample includes a large number of local metal-poor galaxies, we find that our target's EW(Hβ) corresponds to their "medium-EW" subsample, giving an inferred metallicity of $12 + \log(\mathrm{O/H}) = 7.15 \pm 0.20$. Although different calibrations introduce systematic offsets of up to a few tenths of a dex, the conclusion that our source is an extremely metal-poor galaxy remains unaffected.

CAPERS-39810 therefore represents another JWST-confirmed extremely metal-poor galaxy at intermediate redshift, following the recent discoveries reported by Cai *et al.* (2025) and Vanzella *et al.* (2025) (see Figure 3). Its detection extends the census of EMPGs to the redshift range between local analogs and the numerous metal-poor systems now uncovered at $z \gtrsim 6$ (Hsiao *et al.* 2025; Willott *et al.* 2025; Cullen *et al.* 2025; Morishita *et al.* 2025; Nakajima *et al.* 2025). Such extremely metal-poor systems may in fact be common throughout the Universe. However, current observational constraints make them particularly difficult to identify at intermediate redshifts. The limited survey volume of existing NIRSpec programs, the low signal-to-noise ratio at the blue end of the prism spectra, the intrinsically faint nature of EMPGs, and the high observational cost of grating spectroscopy have collectively restricted systematic studies of EMPGs around the cosmic noon. Expanding the census of such galaxies in this epoch is essential for tracing the chemical enrichment history of the Universe, as it directly probes the conditions under which the first generations of metal-poor stars continue to form in low-mass systems.

References

Sanders, R. L., Shapley, A. E., Topping, M. W., Reddy, N. A., & Brammer, G. B. (2024). Direct Te-based metallicities of z= 2–9 galaxies with JWST/NIRSpec: empirical metallicity calibrations applicable from reionization to cosmic noon. The Astrophysical Journal, 962(1), 24.

Nakajima, K., Ouchi, M., Xu, Y., Rauch, M., Harikane, Y., Nishigaki, M., ... & Zahedy, F. S. (2022). EMPRESS. V. Metallicity diagnostics of galaxies over 12+ log (O/H) ≃ 6.9–8.9 established by a local galaxy census: preparing for JWST spectroscopy. The Astrophysical Journal Supplement Series, 262(1), 3.

Scoville, N., Aussel, H., Brusa, M., Capak, P., Carollo, C. M., Elvis, M., ... & Tyson, N. D. (2007). The cosmic evolution survey (COSMOS): overview. The Astrophysical Journal Supplement Series, 172(1), 1.

Bushouse, H., Eisenhamer, J., Dencheva, N., et al. 2025, JWST Calibration Pipeline (1.17.1). Zenodo.

Carnall, A. C., McLure, R. J., Dunlop, J. S., & Davé, R. (2018). Inferring the star formation histories of massive quiescent galaxies with BAGPIPES: evidence for multiple quenching mechanisms. Monthly Notices of the Royal Astronomical Society, 480(4), 4379-4401.

Salim, Samir, et al. "Dust Attenuation Curves in the Local Universe: Demographics and New Laws for Star-Forming Galaxies and High-Redshift Analogs." The Astrophysical Journal, vol. 859, no. 1, 17 May 2018, p. 11, https://doi.org/10.3847/1538-4357/aabf3c.

Shuntov, M., Akins, H. B., Paquereau, L., Casey, C. M., Ilbert, O., Arango-Toro, R. C., ... & Yang, J. (2025). COSMOS2025: The COSMOS-Web galaxy catalog of photometry, morphology, redshifts, and physical parameters from JWST, HST, and ground-based imaging. arXiv preprint arXiv:2506.03243.

Casey, C. M., Kartaltepe, J. S., Drakos, N. E., Franco, M., Harish, S., Paquereau, L., ... & Zavala, J. A. (2023). COSMOS-Web: an overview of the JWST Cosmic Origins Survey. The Astrophysical Journal, 954(1), 31.

Koekemoer, A. M., Aussel, H., Calzetti, D., Capak, P., Giavalisco, M., Kneib, J. P., ... & Shopbell, P. L. (2007). The cosmos survey: Hubble space telescope advanced camera for surveys observations and data processing. The Astrophysical Journal Supplement Series, 172(1), 196.

Cai, S., Li, M., Cai, Z., Wu, Y., Yu, F., Dickinson, M., ... & Zou, J. (2025). A Metal-Free Galaxy at $z = 3.19$? Evidence of Late Population III Star Formation at Cosmic Noon. arXiv preprint arXiv:2507.17820.

Nakajima, K., Ouchi, M., Harikane, Y., Vanzella, E., Ono, Y., Isobe, Y., ... & Zhang, Y. (2025). An Ultra-Faint, Chemically Primitive Galaxy Forming at the Epoch of Reionization. arXiv preprint arXiv:2506.11846.

Vanzella, E., Messa, M., Zanella, A., Bolamperti, A., Castellano, M., Loiacono, F., ... & Meneghetti, M. (2025). A Pristine Star-Forming Complex at z= 4.19. arXiv preprint arXiv:2509.07073.

Hsiao, T. Y. Y., Sun, F., Lin, X., Coe, D., Egami, E., Eisenstein, D. J., ... & Zhu, Y. (2025). SAPPHIRES: Extremely Metal-Poor Galaxy Candidates with $12 + \log(\mathrm{O/H}) < 7.0$ at $z \sim 5 - 7$ from Deep JWST/NIRCam Grism Observations. arXiv preprint arXiv:2505.03873.

Willott, C. J., Asada, Y., Iyer, K. G., Judez, J., Rihtarsic, G., Martis, N. S., ... & Tripodi, R. (2025). In Search of the First Stars: An Ultra-Compact and Very Low Metallicity Lyman-α Emitter Deep Within the Epoch of Reionization. arXiv preprint arXiv:2502.07733.

Cullen, F., Carnall, A. C., Scholte, D., McLeod, D. J., McLure, R. J., Arellano-Córdova, K. Z., ... & Stevenson, S. (2025). The JWST EXCELS survey: an extremely metal-poor galaxy at z= 8.271 hosting an unusual population of massive stars. Monthly Notices of the Royal Astronomical Society, 540(3), 2176-2194.

Morishita, T., Liu, Z., Stiavelli, M., Treu, T., Bergamini, P., & Zhang, Y. (2025). Pristine Massive Star Formation Caught at the Break of Cosmic Dawn. arXiv preprint arXiv:2507.10521.

Mondal, C., Saha, K., Borgohain, A., Smith, B. M., Windhorst, R. A., Reddy, N., ... & Jansen, R. A. (2025). GNHeII J1236+ 6215: A He II λ1640 emitting and potentially LyC leaking galaxy at z= 2.9803 unveiled through JWST & Keck observations. arXiv preprint arXiv:2506.06831.

Sanders, R. L., Shapley, A. E., Reddy, N. A., Kriek, M., Siana, B., Coil, A. L., ... & Barro, G. (2020). The MOSDEF survey: direct-method metallicities and ISM conditions at z$\sim$1.5–3.5. Monthly Notices of the Royal Astronomical Society, 491(1), 1427-1455.

Chakraborty, P., Sarkar, A., Smith, R., Ferland, G. J., McDonald, M., Forman, W., ... & Grant, C. (2025). Unveiling the Cosmic Chemistry. II."Direct" Te-based Metallicity of Galaxies at 3$<$ z$<$ 10 with JWST/NIRSpec. The Astrophysical Journal, 985(1), 24.

Scholte, D., Cullen, F., Carnall, A. C., Arellano-Córdova, K. Z., Stanton, T. M., Barrufet, L., ... & Zou, H. (2025). The JWST EXCELS survey: probing strong-line diagnostics and the chemical evolution of galaxies over cosmic time using Te-metallicities. Monthly Notices of the Royal Astronomical Society, 540(2), 1800-1826.

Kroupa, P., & Boily, C. M. (2002). On the mass function of star clusters. Monthly Notices of the Royal Astronomical Society, 336(4), 1188-1194.

Calzetti, D., Armus, L., Bohlin, R. C., Kinney, A. L., Koornneef, J., & Storchi-Bergmann, T. (2000). The Dust Content and Opacity of ActivelyStar-forming Galaxies. The Astrophysical Journal, 533(2), 682.